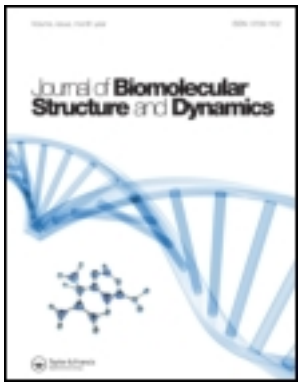

Journal of Biomolecular Structure and Dynamics
Publication details, including instructions for authors and subscription information:
http://www.tandfonline.com/loi/tbsd20

K^+ and Na^+-Induced Self-Assembly of Telomeric Oligonucleotide $d(TTAGGG)_n$

Xiao-Yan Zhang [a], En-Hua Cao [a], Yan Zhang [a], Chunqing Zhou [b] & Chunli Bai [b]
[a] Centre for Molecular Biology, Institute of Biophysics Chinese Academy of Sciences, 15 Datun Road, Chaoyang District, Beijing, 100101, P. R. China
[b] Center for Molecular Sciences, Institute of Chemistry Chinese Academy of Sciences, Beijing, 100080, China
Version of record first published: 15 May 2012.

To cite this article: Xiao-Yan Zhang , En-Hua Cao , Yan Zhang , Chunqing Zhou & Chunli Bai (2003): K^+ and Na^+-Induced Self-Assembly of Telomeric Oligonucleotide $d(TTAGGG)_n$, Journal of Biomolecular Structure and Dynamics, 20:5, 693-701

To link to this article: http://dx.doi.org/10.1080/07391102.2003.10506886

Journal of Biomolecular Structure & Dynamics, ISSN 0739-1102
Volume 20, Issue Number 5, (2003)

K^+ and Na^+ -Induced Self-Assembly of Telomeric Oligonucleotide $d(TTAGGG)_n$

http://www.jbsdonline.com

Xiao-Yan Zhang[1]
En-Hua Cao[1,*]
Yan Zhang[1]
Chunqing Zhou[2]
Chunli Bai[2]

[1]Centre for Molecular Biology
Institute of Biophysics
Chinese Academy of Sciences
15 Datun Road, Chaoyang District
Beijing 100101, P. R. China
[2]Center for Molecular Sciences
Institute of Chemistry
Chinese Academy of Sciences
Beijing 100080, China

Abstracts

The telomeric DNA oligomers, $d(TTAGGG)_n$, where n=1, 2, 4, could self-associate into the multi-stranded structures in appropriate condition and exhibited a different CD spectra. The present of Na^+ was more advantage to facilitate the formation of anti-parallel conformation, but the present of K^+ enhanced their thermal stability. Spectroscopic analysis of 3, 3´-diethyloxadicarbocyanine (DODC) showed the formation of hairpin quadruplex structures for $d(TTAGGG)_2$ and $d(TTAGGG)_4$, but d(TTAGGG) could not. The four-stranded tetraplexes and branched nanowire formed in the present of K^+ or Na^+ alone were observed by atomic force microscopy (AFM). The ability to self-assemble of $d(TTAGGG)_n$, into four-stranded tetraplexes and nanowires depends strongly on the number of repeating units and ionic environment. A model to explain how these structures formed is proposed.

Key words: telomeric DNA, nanowire structure; quadruplex, monovalent cations, circular dichroism, atomic force microscopy.

Introduction

Telemetric DNA oligomers containing guanine-rich repeats can self-associate in the aqueous solution to form highly ordered structures include quadruplexes and wires according to the sequence and environmental effects (1-5). Of these structures, four-stranded DNA complexes have been studied most extensively (6-9). These structures exhibit distinguishing chemical (1), spectroscopic (10-12), and physical properties (13, 14). Since all these structures readily occur under the physiologically compatible conditions of pH, temperature and ion strength, they have been presumed to play an important functional role in various biological processes that involve DNA (15-17). Proposals regarding these functions include transcription regulation, gene recombination as well as chromosome organization and packing (18-20). Therefore, a detailed investigation of these structures not only is required for our elucidating their potential functions, but also can provide us an insight into the intrinsic mechanism underlying these genetic diseases. Moreover, such understanding can further help us to design some rational oligonucleotides for specific therapeutic, diagnostic and other biotechnological applications (21).

Some studies have shown that the nature of the complex formed by an oligonudeotide depends in part on the base sequence and strong depends on the monovalent cations, such as K^+ and Na^+ (22-24). Evidence suggests that K^+ is much more effective in stabilizing G-quadruplex formation (7), and that for contiguous guanine oligomers, the parallel strand orientation is thermodynamically more favorable than the antiparallel orientation in the G-quadruplex formation (4, 6) found that the telomeric oligonicleotide d(GGGGTTGGGG) could form four-stranded tetraplexes and branched nanowire. Recently, it was further found that the guanine rich sequence d(GGCGTTGCGG) can forms branch structure and long

*Phone: +86-10-64888567
Fax: +86-10-64871293
Email: caoeh@sun5.ibp.ac.cn

DNA nanowire (25). On other hand, a lot of success's case demonstrated atomic force microscopy (AFM) method can be used to determine DNA structure to allow accurate measurement of dimensions. In the developed tapping mode AFM, reduced lateral forces result in better sample preservation and higher resolution images. Most importantly, the accurately measured height information is critically important for the evaluation of DNA higher-order structure (26, 27).

In this work, we used Circular Dichroism (CD) and Atomic Force Microscopy (AFM) to study the structural properties of the K^+ and Na^+ complexes of the three sequences of $d(TTAGGG)_n$ (where n=1, 2, 4). Results indicated that the ability to self-assemble of $d(TTAGGG)_n$ into four-stranded tetraplexes and nanowires depends strongly on the number of repeating units and ionic conditions.

Materials and Methods

DNA Oligonucleotides

All the oligodeoxynucleotides were obtained from Life Technologies, Inc. (LTI, Hong kong). Purification and desalination were performed by reverse HPLC (C-18). The purity was determined to meet the experimental requirement by the UV spectrum. λ-DNA is used as a reference of duplex DNA.

Preparation of Noncovalent Complexes

Oligodeoxynucleotides were solved in a 10 mmol/L Tris-HCl (pH=7.5) buffer containing a certain concentration of KCl and NaCl, respectively. Samples were heated at 80° C for 5-10 min, then cooled slowly to room temperature, and then incubated at 4° C for 5-6 h.

CD Spectrum Analysis

CD spectra were made by a Jasco J-720 spectropolarimeter. Samples were measured at room temperature with use of special cells. (All measurement is done at room temperature unless specified.) The instrument conditions were as follows: scan range, 320-200 nm; scan speed, 100 nm/min; quartz cell length, 1 mm; sensitivity, 5 mdeg; response, 4 s; resolution, 1 nm; accumulation times, 4; temperature, 20° C; reference sample, buffer solution containing the same cation condition. Sample temperature was controlled by an external circulating water bath. All CD spectra were averaged over 8 acquisitions with a scan rate of 50 nm/min and a time constant of 1 s. All CD data were baseline corrected for signals due to the cell and buffer.

Spectroscopic Analysis of Hairpin Quardruplexes

Spectroscopic analysis of hairpin quardruplexes was carried out on a Hitach U-3200 spectrophotometer according to the methods described by Chen *et al*. (28). Oligodeoxynucleotides were solved in 1mM Tris-HCl (pH 7.5), and stored at -20° C. A stock solution of 3, 3´-diethyloxadicarbocyanine (DODC, Sigma Chemical Co.) was prepared in methanol. Stock solutions of Tris-HCl buffer, DODC, NaCl, and oligodeoxynucleotide were mixed. Final buffer concentrations were 10mM Tris-HCl and 150 mM NaCl (pH 7.5). The DODC concentration was below 6 μM, while the concentrations of DNA samples ranged from 10 to 36 μM.

Atomic Force Microscopy Imaging

A drop of sample (about 2 μL, 10 μg/ml) was spotted on freshly cleaved mica and left to stabilize about 2 min. Before washing the salt by super pure water (Millipore) the sample was dried by compressed N_2. Imaging was performed in tapping mode with a Nanoscope III (Digital Instruments), using a 125 μm Si tapping tip. The λDNA was dissolved in the same buffer as the three G-rich sequences.

The UV experiments were carried out on a Hitach U-3200 spectrophotometer, Cells with optical path-lengths of 10 mm were used and the temperature of the cell holder was controlled by an external circulating water bath. The UV melting experiments were done at a heating rate of 0.25° C/ min, monitoring the absorption change at 260 and 280 nm.

Results and Discuss

CD Spectrum Analysis

CD spectra can inspect the formation of G-quadruplex. There are two basic kinds of CD spectra usually observed for telomeric DNAs (29), one form exhibits a positive CD band at ~265 nm and a negative band at ~240 nm (type I), while the other form exhibits a positive band at ~295 nm and a negative band at ~260 nm (type II). The parallel quadruplex structure (linear conformation) exhibits as type I. but the antiparallel quadniplex (folded conformation) does as type II. As shown in Figure 1A. Samples A_0, B_0 and C_0 exhibited a type I CD spectrum as judged by a characteristic signature with 265 nm positive and 240 nm negative bands. There were faint positive bands at around 290 nm in curves of B_0 and C_0, due to the formation of intramolecular or intermolecular hairpin dimer quadruplexes when repetitive frequency n was 2 or 4. However, the proportion was quite low and increased with the increase of repetitive frequency.

The CD spectra of complex of d(TTAGGG)$_4$ with Na^+ were shown in Figure 1B, it's CD spectra exhibits a CD spectrum of type II with a 295 nm positive peak, a 260 nm negative valleys. DNA becomes an antiparallel quadruplex conformation with increase of sequence length (30). But contrary to Na^+, the addition of K^+ made these curves exhibited double positive bands between 260-290 nm. The CD spectra of complex of d(TTAGGG)$_n$ with K^+ in Figure 1C exhibits a CD spectrum of neither type II nor type I with a 290 nm positive peak, a 240 nm negative valleys. It indicates that K^+ can stabilize G-quartets both in parallel and anti-parallel structures, it is possible that the two conformations coexist in the same solution and give the special spectra. This is in accordance with the results reported in reference (31). It is obvious that the addition of K^+ can change the structures of oligonucleotide notably and has different effects on sequences in different length, the longer the sequence is, the greater the change will be.

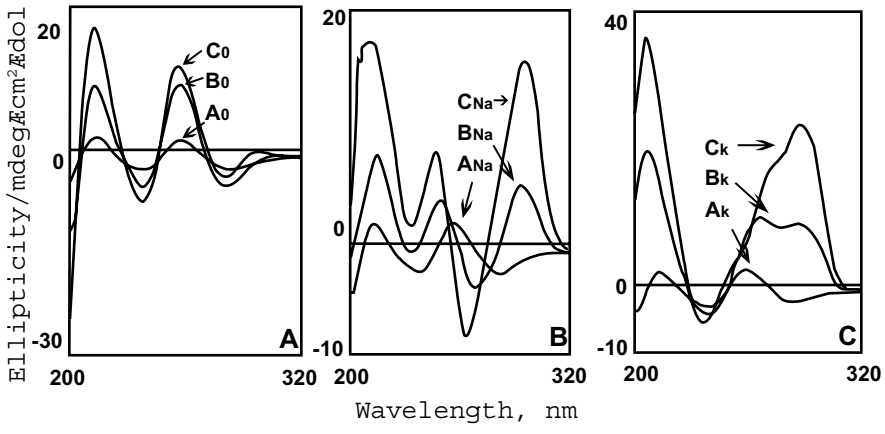

Figure 1: CD spectra of (A) d(TTAGGG), (B) d(TTAGGG)$_2$ and (C) d(TTAGGG)$_4$ in Tris-HCl buffer at 20° C, pH 7.5. (a) without K^+ and Na^+; (b) with 80 mmol/L Na^+; (c) with 80 mmol/L K^+.

Spectroscopic Analysis of Hairpin Quardruplexes

Figure 2 showed that the visible absorbance spectrum of DODC at low concentration has a maximum at 576 nm with a small shoulder at 530-550 nm and a relative intensity ratio of A576/A536≈3.1. Addition of (TTAGGG)$_2$ and (TTAGGG)$_4$ in the

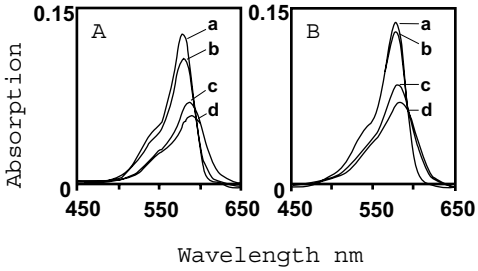

Figure 2: Absorbance spectra of 1μM DODC in 10mM Tris-HCl containing 80 mM KCl (A) or containing 150 mM NaCl (B). Telomeric oligonucleotide: 10 μM strands. a, without DNA; b, d(TTAGGG); c, $d(TTAGGG)_2$; d, $d(TTAGGG)_4$.

present of Na^+ or K^+ resulted in a decrease and small red shift for the 576 nm peak. But addition of d(TTAGGG) had not any effect on site of the 576 nm peak and relative intensity ratio of A576/A536. It further evidences that $d(TTAGGG)_2$, $d(TTAGGG)_4$ could self-assemble into hairpin quadruplex structures (corresponding G2-DNA and G1-DNA in Fig. 5B and C), TTAGGG does not form the hairpin quadruplex structures (corresponding G4-DNA in Fig. 5A) under same conditions (28). From Figure 2 we can see the effect of K^+ was more strong than that of Na^+ in the decrease and red shift for the 576 nm peak, this is because K^+ can stabilize G-quartets both in parallel and anti-parallel structures, only an antiparallel quadruplex conformationwith for Na^+. This is in accordance with above CD results.

Analysis of Melting Profiles

As showed in Table I, it can be seen that the T_m of $d(TTAGGG)_4$ was higher than that of $d(TTAGGG)_2$. Addition of Na^+ and K^+ increased T_m of $d(TTAGGG)_2$ and $d(TTAGGG)_4$, and T_m in the present of K^+ is higher than one in the present of Na^+. It was found that T_m value at 280 nm was higher than that of at 260 nm.

The different of T_m values determined at different wavelengths is not surprised. Possible reason is related to quadruplex structure formed in the present of monovalent cation. We surely find that qudraplexes in this range 270-320 nm, especially at 280 nm differ from duplex, showing a little higher absorbance than the duplex forms. In general, the UV-absorption spectra of the duplex, triplex and quadruplex DNA in the region of 240-280 nm are quite similar. However, if observed carefully, some subtle changes among them can be found such as for the quadruplex. The qudraplexe DNA in this range at 270-320 nm show a little higher absorbance than the duplex forms (11, 32). Zahler *et al*. (19) reported to exhibit two overlapping peaks in the 260-280 nm region. Thermal denaturation studies can provide the information of DNA stability. The energy required to rupture the base pairs of GC, AT , GG and AA should be different. For the quadruplex (or triplex) DNA, the melting is accompanied by a hyperchromic absorbance change at 284 nm, whereas denaturation of the duplex is not (33, 34). It is this reason, thus, thermal denaturation of quadruplex DNA was monitored by the absorbance at 270-320nm, not at 260 nm (19, 32, 35). It is obvious that it is related to quadruplex structure formed in the present of monovalent cation.

Table I
Tm value of sequence d $(TTAGGG)_2$ and d $(TTAGGG)_4$

Ion	Tm			
	$d(TTAGGG)_2$		$d(TTAGGG)_4$	
	260nm	280nm	260nm	280nm
Control (No ion)	42.08	43.02	55.81	54.69
Na^+	44.81	46.30	53.22	56.07
K^+	45.32	56.27	66.53	67.05

Ion concentration is 80 mM, sequences concentration is 50μM.

Atomic Force Microscopy Image

AFM images showed the λ-DNA molecule alone was an extended line state (Fig. 3A, B and C), it is about 0.58 ± 0.23 nm height and 12 nm width, corresponding to a typical double stranded DNA tractate (36). The histogram of height distribution was shown in Figure 4A, B.

G-DNA, G-wires, and G-branches can be seen in the AFM images of Figure 3. The spheres (about 30.23 nm diameter and 1.45 nm height) showed in Figure 2D-L d are the images of d(TTAGGG), $d(TTAGGG)_2$ and $d(TTAGGG)_4$ aggregates into G-DNA (corresponding G4-DNA in Fig. 5A). However, $d(TTAGGG)_2$ and $d(TTAGGG)_4$ were self-assembled in parallel to the folded structure first, and then aggregated into the spheres (corresponding G2-DNA, G1-DNA in Fig. 5B and C).

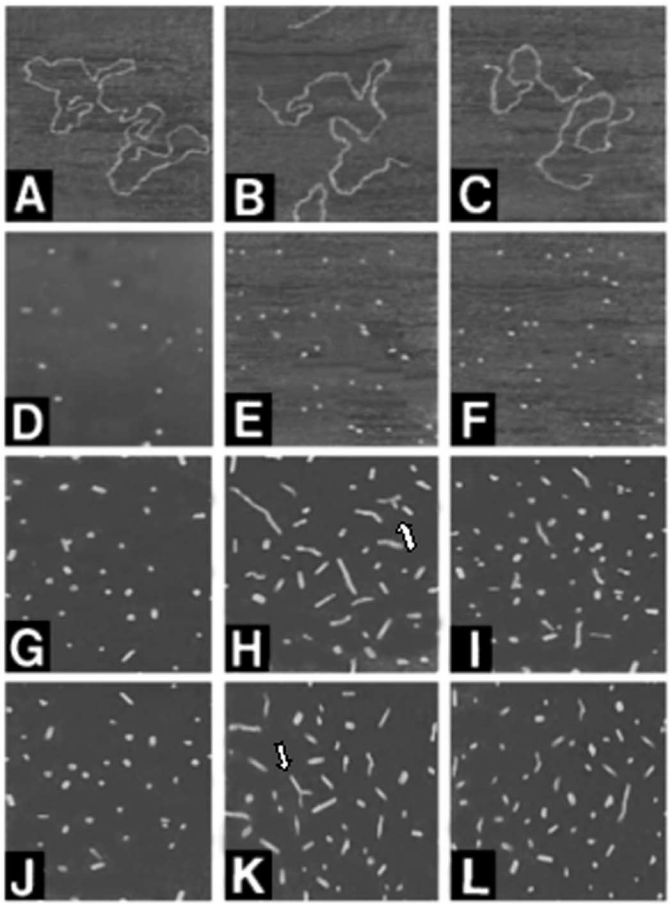

Figure 3: AFM images of aggregates formed by $(TTAGGG)_n$ in Tris-HCl buffer, pH 7.5 with different ionic condition: Na^+ or K^+ is absent (left panele), 80mM Na^+ (middle panel), 80mM K^+ (right panel). A-C, λ-DNA plasmid DNA; D-F, d(TTAGGG); G-I, $d(TTAGGG)_2$; J-L, $d(TTAGGG)_4$. Scan bars are A-C: 3000×3000; D-L: 5000×5000 nms.

The different length lines (not sphere) showed in Figure 3H, I, K and L was topic images of $d(TTAGGG)_2$ and $d(TTAGGG)_4$ aggregates into G-wires (corresponds G4- wires G8- wires in Fig. 5). The relative fraction of nanowires increases with the number of repeated sequences and addition of Na^+ or K^+. Three maggot-like branch crossing at the same point (indicated by an arrow) showed in Figure 3H, K is topic images of $d(TTAGGG)_2$ and $d(TTAGGG)_4$ aggregates into G-branches (corresponds G4- branches in Fig. 5). It should be noted that it showed different structure state including G-DNA, G-wires, and G-branches in Figure 3H, I, K and L. The very long nanowires and web structure of GGCGTTTTGCGG found in our previous work (25) could not be found in the work. Clearly, the number of d(TTAGGG) and Na^+ and K^+ plays an important role in the stability of the aggregated species (37). AFM images support above spectroscopic results and reveal the morphologies of these aggregates.

The nanowires found in the present of Na^+ or K^+ (in Fig. 3) had different apparent height. The histogram graphs of the height of these DNA nanowires were shown in Figure 4. The height of the G quadruplex should be the different from that of B DNA, as measured by the same technique. Experimental evidences have be presented (27). AFM studies have revealed that the height of duplex DNA is half that of triplex DNA and almost one quarter of that of quadruplex DNA, suggesting that the higher the DNA, the more strands it has (4). The wire formed by $d(TTAGGG)_2$ and $d(TTAGGG)_4$ in the present of Na^+ or K^+ both were two to three times greater than the height of λDNA. These data suggest that the height of G-wires depends upon the sequence and Na^+ or K^+ in the same growth conditions, K^+ was more advantage to facilitate the forming of complex wires, as G8- wires (Fig. 5). Marsh, *et al*. (4) found that the range of the length of G-wires formed by d(GGGGTTGGGG) is from 10 to >1000 nm, but the height and width of wires appeared to be uniform, ranging from 1.27 to 2.39 nm. Sha *et al*. (30) showed $d(XGG)_4$ can form the wires in the present of K^+, but replacement of K^+ by Na^+ fails to induce a similar phenomenon. Vesenka *et al*. (37) have measured G-wire's

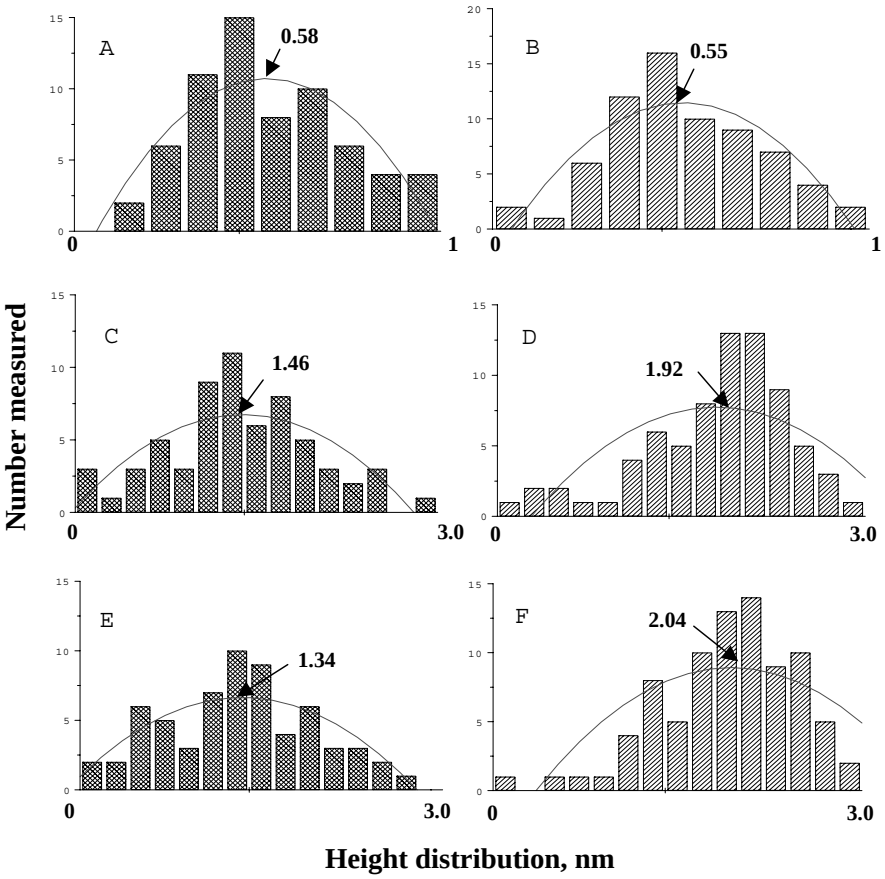

Figure 4: Statistics of the AFM measurement of the nanowires seen in Figure 3. The histogram of the distribution of plasmid DNA's height (A, B), the nanowires formed by $d(TTAGGG)_2$ (C, D), the nanowires formed by $d(TTAGGG)_4$ (E, F), 80mM Na^+ (left panel), 80mM K^+ (right panel).

height, and the height of those G-wires is 2.0 ± 0.5 nm. However, no direct evidence proves those wires are four strand wires. Now in our results, we found the height of wire for Na^+ is lower than 2.0 nm, the height of wire for K^+ is higher than 2.0 nm, but both much higher than the λDNA. It is possible a four strand wire, and the higher wires are more complex wires, which is similar our previous work (25). In this work, the long nanowires and web structure could not be found, it maybe related with the lack of Mg^{2+}, the presence of $MgCl_2$ in solutions appears to elongate the-induced aggregates (4, 38, 39).

AFM images maybe affected by many factors, such as hydrophobic nature of the guanines. Several studies (40, 41) have demonstrated that i) in extremely diluted solution (~1 ng/μl or below), long DNA molecules undergo a monomolecular collapse; ii) in very dilute solution (~10 ng/μl or below), microaggregates form with short or long molecules and remain in suspension; and iii) in dilute solutions (~1 mg/ml), large aggregates are formed that sediment readily. Base on these, we observed the morphology change of DNA molecules by varying the concentration from 50 ng/μl to 1 ng/μl and examined the intermediate structures during this process. When DNA concentration was diluted to 10 ng/μl, a large complex network structure appeared (42), so in this work, the DNA concentration used was chosen at 10 ng/μl. Thus, it is not under highly concentrating conditions used in AFM experiments. On other hand, to avid the G rich strands aggregate in aqueous solution due to their tendency to club together/hydrophobic nature, to effect the formation of order structure, samples were heated at 80° C for 5-10 min, then cooled slowly to room temperature, and then incubated at 4° C for 5-6 h. It should be advantage to formation of their finer structure.

The different effect of K^+ and Na^+ on the height of wire was observed, however, the effects of sequence lengths were minor. Probably, the spaces inside the G-quar-

tets of different conformations are different in size and need cations of variety diameters to stabilize them. After all, there is no perfect explanation to this phenomenon yet; more research work needs to be done.

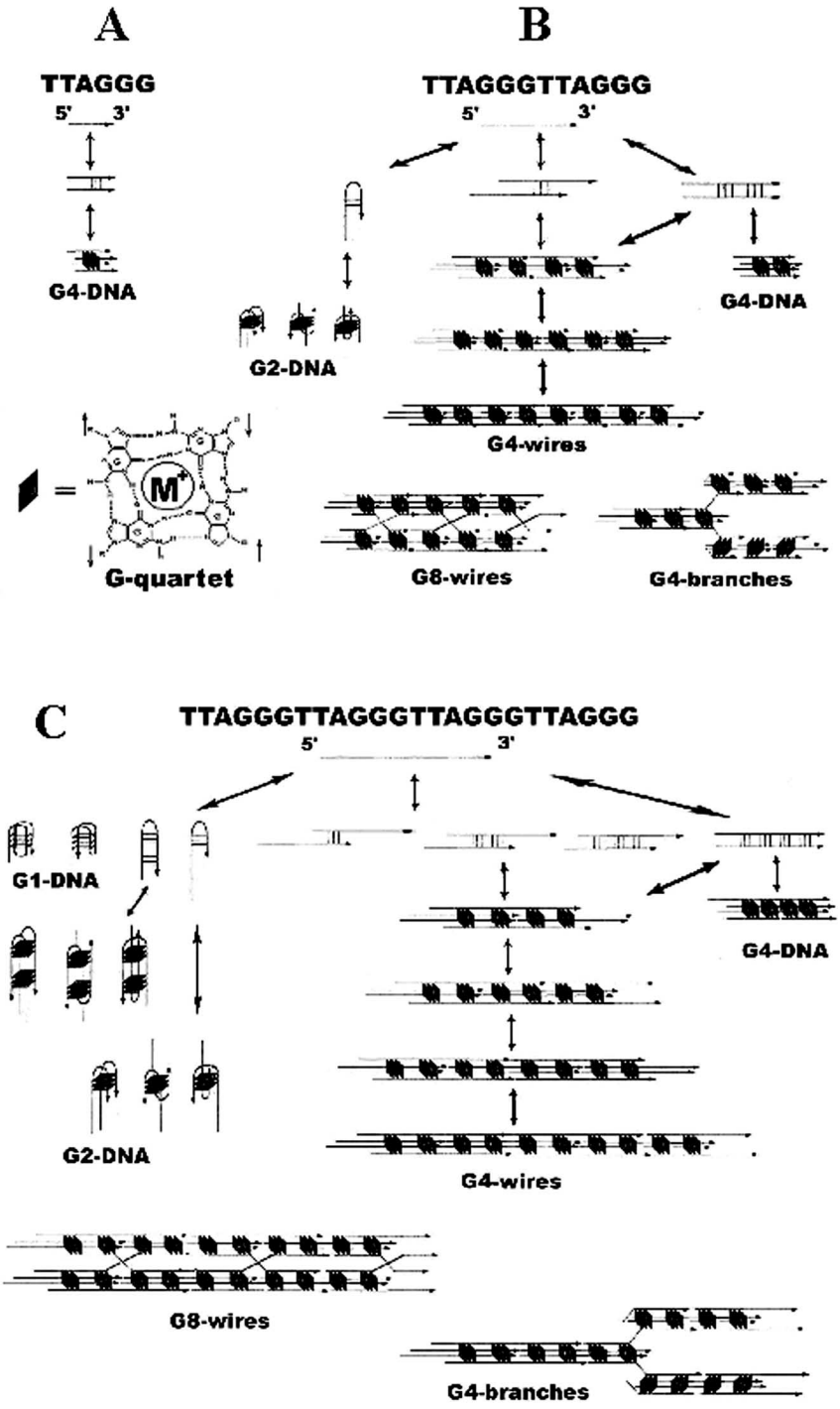

Figure 5: The pathways of d(TTAGGG)$_n$ do self-assembly. A, d(TTAGGG); B, d(TTAGGG)$_2$; C, d(TTAGGG)$_n$.

Alternative pathways of structure formation of guanine rich oligonucleotides have been proposed (4, 43). It can not account for the quadruplex structure and the different in present of Na^+ or K^+. We propose other alternative pathways too. In these pathways, when n is 1, the sequence can only adopt a kind of intermolecular quadruplex structure (corresponding G4-DNA in Fig. 5A). Its CD spectra showed as type I. When n is 2, it can also form intermolecular hairpin structure (corresponding G4-DNA in Fig. 5B), then dimerize into anti-parallel conformation and nanowires (corresponding G4-wires in Fig. 5B). While n increases to 4, it is even able to fold itself into monomolecular quadruplexes structure (corresponding G4-DNA in Fig. 5C), its CD spectra showed as type II, and nanowires (corresponding

G4-wires in Fig. 5C). In fact, there is equilibrium between folded structure and linear structure. But the equilibrium is reached over a long period of time due to the extremely slow kinetics of formation / dissociation which typical for four-stranded quadruples. If linear structure formed, once metal ions were added into solutions, they interacted with oligonucleotide sequence and advantaged to convert them into more thermodynamically stable structures. In a word, the longer a sequence is, the more complicated the case may be; the more complicated the case is, the greater effects cations may have. In general, if n>2, the linker $d(TTAGGG)_n$ can form a loop (43). We assume that the T_2A can form a loop in d(TTAGGGTTAGGG) or d(TTAGGGTTAGGGTTAGGGTTAGGG) as in Figure 5, so the branched structure can be formed (corresponding G4-branches in Fig. 5B and C). We assume that one strand of the G4-wire quadruplex is cross to another G4-wire and vice versa, this structure is greatly similar to the parallel Holliday junction if we regard other three strands of quadriiplex as the side strand of the Holliday junction, then a G8-wire formed (corresponding G8-wires in Fig. 5B and C). Similarly more complex G-wire could be formed.

By using CD and AFM, we found a special guanine rich sequence $d(TTAGGG)_n$ can form quadriiplex DNA. The ability to self-assemble into wires not only clearly demonstrate its potential as scaffold structures for nano-technology, but also give aids to understand telomeric structure further.

Acknowledgement

This work was supported by a grand from National Science Foundation of China. (30170246, 90206041) and the Chinese Academy of Sciences (5-121111-05).

References and Footnotes

1. Gusclilbauer, W., Chantot, J., Thiele, D. *J. Biomol. Struct. Dynamics 8*, 491-51 (1990).
2. Williamson, J. R. *Annu. Rev. Biophys. Biomol. Struct. 23*, 703 (1994).
3. Poon, K., Macgregor, R. B. *Biophys. Chem. 84*, 205-216 (2000).
4. Marsh, T., Vesenka, C. J., Henderson, E. *Nucleic Acids Res. 25*, 696-700 (1995).
5. Chen, A., Cao, E. H., Sun. X. G., Qin. J. F. *Surface and Interface Analysis 32*, 32-37 (2001).
6. Sen, D., Gilbert, W. *Nature 334*, 364-366 (1988).
7. Lu, M., Guo, Q., Kallenbach, N. R. *Biochemistry 32*, 508-60l (1993).
8. Dai, T., Marotta, S. P., Sheardy, R. D. *Biochemistry 34*, 3655-3662 (1995).
9. Harrington, C., Lan, Y., Akman, S. A. *The Journal of Biological Chemistry 272*, 24631 (1997).
10. Poon, K, Macgregor, R. B. *Biopolymers 45*, 427-434 (1998).
11. Sun, X. G., Cao, E. H., He, Y. J. *J. Biomol. Struct. Dynamics 16*, 863-869 (1999).
12. Protozanova, E., Macgregor, R. B. *Biophys. J., 75*, 982-989 (1998).
13. Jin, R., Gaffney, B. L , Wang, C., Jones, R. A., Breslauer, K. J. *Proc. Natl. Acad. Sci. USA 89*, 8832-8836 (1992).
14. Poon, K., Macgregor, R. B. *Riophys. Chem. 79*, 11-23 (1995).
15. Blackburn, E. H., *Nature 408*, 53-56 (1999).
16. Cao, E. H., Sun, X. G., Zhang, X. Y., Qin, J. F., Liu, D., Wang, C., Bai, C. L. *J. Biomol. Struct. Dynamics 17*, 871-878 (2000).
17. Simonsson, T., Pecinka, P., Kabista, M. *Nucleic Acids Res. 26*, 1167-1172 (1998).
18. Klapper, W., Parwaresch, R., Krupp, G. *Mechanisms of Aging and Development 122*, 695-712 (2001).
19. Zahler, A. M., Williamson, J. R., Cech, T. R., Prescott, D. M. *Nature 350*, 718-720 (1991).
20. Johnson, F. B., Marciniak, R. A., Guarente, L. *Curr. Opinion in Cell Biology 10*, 332 (1998).
21. Huurley, L. H., Wheelhouse, R.T., Sun, D., Kerwin, S. M., Salazar, M., Fedoroff,O. Y., Han, F. X., Han, H., Izbicka, E., Von Hoff, D. D. *Pharmacology & Therapeutics 85*, 141-158, 2000.
22. Willimson, J. R., Raghuraman, M. K., Cech, T. R. *Cell 59*, 871 (1989).
23. Hardin, C. C., Henderson, E., Watson, T., Prosser, J. K. *Biochemistry 30*, 4460-4472 (1991).
24. Marotta, S. P., Tamburri, P. A. Sheardy, R. D. *Biochemistry 35*, l0484-10492 (1996).
25. Zhou, C., Tan, Z., Wang, C., Wei, Z., Wang, Z., Bai, C., Qin J., Cao, E. H. *J. Biomol. Struct. Dynamics 18*, 807-812 (2001).
26. Zhong, Q., Inniss, D., Kjoller, K. & Elings, V. B. *Surf. Sci. 290*, L688-L692 (1993).
27. Hansma, H. G., Sinsheimer, R. L., Groppe, J., Bruice, T. C., Elings, V., Gurley, G., Magdalena, B., Mastrangelo, I. A., Hough, P. V. C., Hansma, P. K. *Scanning 15*, 296-299 (1993).
28. Chen, Q., Irwin, D. K., Richard, H. S. *Proc. Natl. Acad. Sci. USA 93*, 2635-9 (1996).
29. Balagunimoorthy, P., Braliniachari, S. K., Mohanty, D., Bansel M. and Sasisekliaran, V. *Nucleic Acids Res. 20*, 061-4067 (1992).

30. Sha, F., Mu, R., Henderson, D., Chen, E. *Biophysical Joumal 77*, 410-423 (1999).
31. Sen, D., Gilbert, W. *Nature 344*, 410 (1990).
32. Chen, F. M. *J. Biol. Chem. 29*, 23090 (1995).
33. Pilch, D. S., Brousseau R., Shafer, R. H. *Nucleic Acids Res. 18*, 5743-5750 (1990).
34. Hansma, H., Revenko,G. I., Kim K. E., Laney, D. *Nucl. Acids Res. 24*, 713-720 (1996).
35. Fang, Y., Bai, C.-L., Zhang, P.-C., Cao, E.-H., He, Y.-J., Tang, Y.-Q. *Science in China (Series B) 37*, 1306-1312 (1994).
36. Hardin, C. C., Corregan, M. J., Liebernan, D. V., Brown, B. A. *Biochemistry 36*, 15428-15450 (1997).
37. Vesenka, J., Marsh, T., Miller, R. and Henderson, E. *J. Vac. Sci. Technol. B 14*, 1413-1417 (1996).
38. Sun, X. G., Cao, E. H., Zhang, X. Y., Liu D. and Bai, C. I. *Inog. Chem. C. 5*, 181-186 (2002).
39. Marsh, T. C., Hendereon, E. *Biochemistry 33*, 10718-10724 (1994).
40. Bloomfield, V. A. *Biopolymers 31*, 1471 (1991).
41. Sikorav, J. L., Pelta, J., Livolant, F. *Biophys J. 67*, 1387-92 (1994).
42. Sun, X. G., Cao, E. H., Liu, M., and Bai, C. I., *Atomic Force Microscopy Chemistry Letters 9*, 981-982 (1999).
43. Sundquist, W. I., Klug, A., *Nature 342*, 825-829 (1989).

Date Received: November 8, 2002

Communicated by the Editor Ramaswamy H Sarma